Electro-thermal model of an integrated buck converter

Baptiste Trajin, Paul-Etienne Vidal, Julien Viven

Electro-thermal model of an integrated buck converter

Baptiste TRAJIN, Paul-Etienne VIDAL, Julien VIVEN
Université de Toulouse; INP; ENI de Tarbes, LGP
47 avenue d'Azereix, BP1629
65016 Tarbes, France
Tel.: +33/ (0) – 562.442.700
Fax: +33/ (0) – 562.442.727
E-Mail: baptiste.trajin@enit.fr

Keywords

«Chopper converter», «Power losses», «Thermal model».

Abstract

This study deals with new integrated systems for power electronic applications including wide-band gap semiconductors. The integration of Silicon carbide (SiC) components provides new perspectives such as higher temperature operating points than conventional Silicon (Si) semiconductors. The present work intends to study the electro-thermal behaviour of an integrated buck converter composed of a Silicon IGBT (Insulated-Gate Bipolar Transistor) and a Silicon carbide diode. An analysis of local heat sources due to Joule effect and compact thermal model of the assembly are proposed to predict local temperature of power electronic components.

Introduction

The emergence of wide-band gap semiconductors allows to design electronic power modules with high compactness and high power density. Indeed, the maturity level of specific components such as those made of Silicon carbide (SiC) and Gallium nitride (GaN) has strongly increased. Nowadays, they may be used for high integrated industrial applications. In order to optimize the overall integration, higher temperature operating points than for conventional Silicon (Si) semiconductors are considered [1]. Consequently, new constrains appear and become critical for power electronics assemblies. Several studies aim at identifying failure modes or critical interfaces [2], [3]. In this field of research, knowledge of the power module operating temperature and even more the temperature experienced by semiconductor devices is of strong interest [4].

Given the difficulties to obtain full controlled SiC semiconductors at low prices, this technology seems to be intended for high voltage applications. On the contrary, uncontrolled SiC semiconductors are already easily accessible and allow to design efficient and optimized conversion functions [5]. Joint use of a classical controlled Si switch and an uncontrolled SiC switch may induce disparities, including thermal ones, in such hybrid assemblies. The main purpose of these study is to intend to study the thermal behaviour of an integrated buck converter composed of a Silicon IGBT and of a Silicon carbide diode. First of all, the characteristics of the electric system are described. Then, a complete theoretical analysis of Joule losses in the different components of the assembly is proposed regarding electric operating point and given geometry and materials. Finally, a thermal model linked to Joule losses is developed and simulation results are provided.

Electric system description

The considered specific integrated function is completed with an external command circuit linked with specific IGBT drivers. The signal experienced by the gate of the IGBT is realized thanks an open loop using a constant duty cycle α. The electrical load of the buck converter is modeled by a constant current source I_{load}. All tests will be performed at low voltage level and nominal current to ensure high thermal dissipation. Figure 1-a illustrates the electric operating diagram and figure 1-b shows the related power electronic assembly. It can be noticed that the power electronic assembly is not encapsulated using a dielectric polymer or an external case in order to simplify thermal models. Power electronic chips are brazed using a Tin-Copper-Silver (Sn-Cu-Ag) alloy on a Silicon nitride Si_3N_4 substrate covered by Copper power tracks. A thin layer of Gold is added on the Copper tracks as a protection against corrosion.

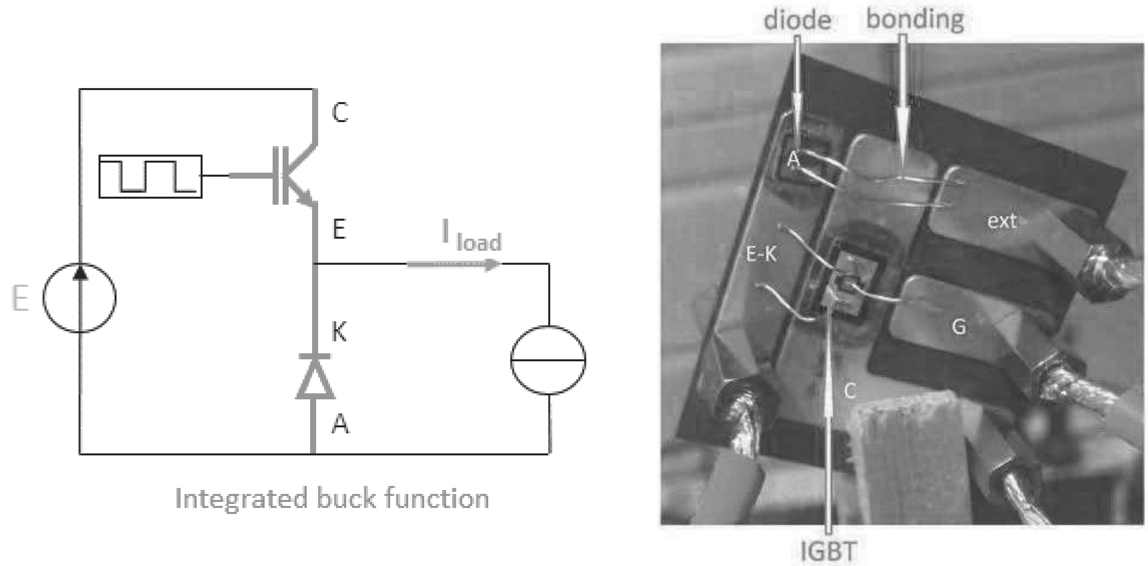

(a) (b)

Fig. 1: Studied electric system

The chopper converter is supplied by a constant adjustable voltage source and the current source load is composed of a series resistance *R* and inductance *L*.

Load current ripple

In this section, it has to be considered that the voltage drops in the semiconductor switches are negligible regarding input voltage. Moreover, the converter is supposed to operate in steady state conditions. Furthermore, assuming that the switching period $T=1/f$ of the converter is lower than the time constant of the electrical load, and that the converter operates in continuous conduction, the amplitude of the current ripple in the load may be expressed by (1) where I_{load} is the average load current.

$$\Delta I_{\text{load}} = (1-\alpha)\cdot\frac{RI_{\text{load}}}{Lf} \tag{1}$$

Given (1), the maximum value of the ripple current is obtained when the duty cycle is *0*. Consequently, the maximum ripple current is equal to $(RI_{load})/(Lf)$. It may be demonstrated that the chopper always operates in continuous conduction if relation $R<Lf$ is verified.

Root Mean Square (RMS) current

Thermal Joule losses are determined by the value of the RMS current in the load. For a switching period, let us consider the current load $i_{load}(t)$ as the summation of a constant part I_{load} and an asymmetrical triangular oscillating component with magnitude of ΔI_{load} (2).

$$
\begin{cases}
i_{\text{load}}(t) = i_{\text{load}} - \dfrac{\Delta I_{\text{load}}}{2} + \dfrac{\Delta I_{\text{load}}}{\alpha T} t, \; t \in [0;\alpha T] \\
i_{\text{load}}(t) = i_{\text{load}} + \dfrac{\Delta I_{\text{load}}}{2} + \dfrac{\Delta I_{\text{load}}\alpha}{(1-\alpha)} - \dfrac{\Delta I_{\text{load}}}{(1-\alpha)} t, \; t \in [\alpha T;t]
\end{cases} \tag{2}
$$

Using (2), it is demonstrated that RMS value of the current $I_{load,\ rms}$ expresses as follows (3).

$$
I_{\text{load, rms}} = \sqrt{\frac{1}{T}.\int_0^T i_{load}^2(t).dt} = \sqrt{I_{load}^2 + \frac{I_{load}^2 R^2 (1-\alpha)^2}{12 L^2 f^2}} \tag{3}
$$

Thus, the RMS load current is approximated by its average value I_{load}. Indeed, resulting error between the RMS current and the previous approximation is then provided by (4). The maximum error is reached for $\alpha=0$.

$$
\varepsilon = \frac{I_{load} R(1-\alpha)}{\sqrt{12} Lf} \tag{4}
$$

System parameters

In this study, the load current is set to $8A$ whatever the duty cycle. It is obtained by acting on the supply voltage E. The load resistance equals $R=1\Omega$ and the load inductance is $L=3mH$. The switching frequency is set to $f=1000Hz$. Regarding (1), the maximum current ripple is $\Delta I_{load}=2.6A$ for $\alpha=0$. It is concluded that the chopper converter always operates in continuous conduction in steady state.

Moreover, regarding (3), the relative error between approximated RMS and averaged currents does not exceed 0.5% as illustrated in figure 2. This study is consistent with the highest oscillations of the load current obtained when the duty cycle tends to 0. So it will be considered in the following that RMS load current is equal to the average load current.

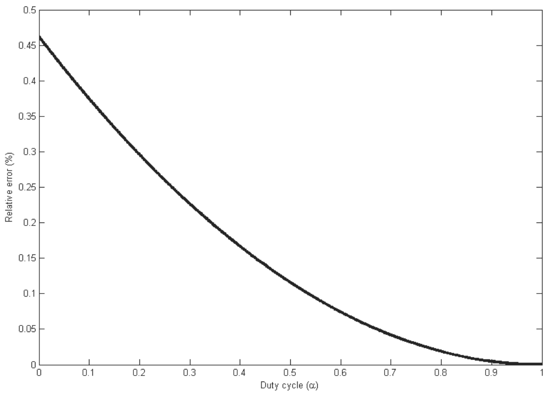

Fig. 2: Relative error on RMS load current

Study of semi-conductors

Voltage drops in semiconductors

In case of forward conduction of an IGBT or a diode, semiconductors are modeled by a cut-in voltage source associated in series with a bulk resistance [6]. Thus, during conduction stage, voltage drops in semiconductors are expressed by (5).

$$
\begin{cases}
v_{\text{igbt}} = v_{\text{ce, sat}} + R_{\text{ds, on}} i(t) \\
v_{\text{diode}} = v_{\text{d0}} + R_{\text{d0}} i(t)
\end{cases} \tag{5}
$$

Regarding the semiconductors used in the system, voltage drops are experimentally determined following *v(i)* measurements in conduction state, for several current values. Results are given in figure 3.

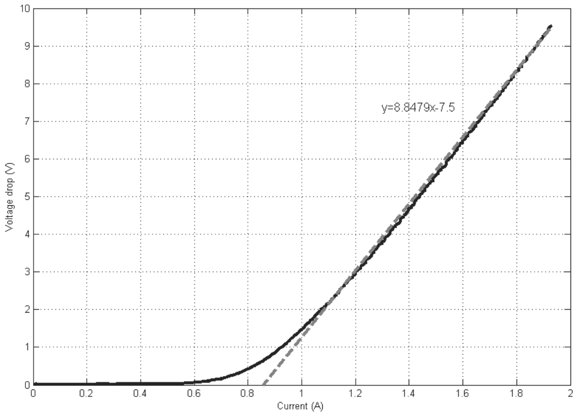

(a) – Si IGBT characteristics

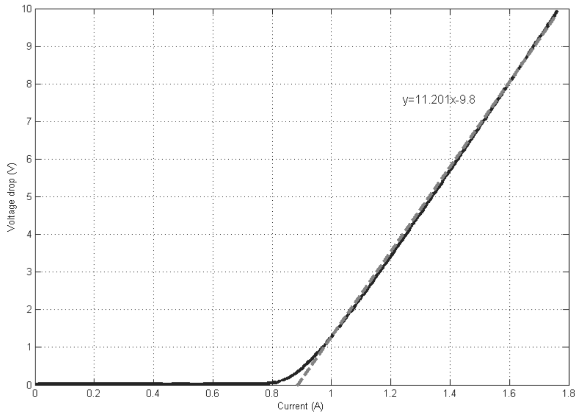

(b) – SiC diode characteristics

Fig. 3: Semiconductors characteristics

This leads to the following values:

- $v_{ce,\ sat}=0.847V$
- $R_{ds,\ on}=0.113\Omega$
- $V_{d0}=0.875V$
- $R_{d0}=0.0893\Omega$

Power losses in semiconductors

Conduction power losses

The power losses in semiconductors during conduction time are estimated through the integral of the product between voltage drop and current over a switching period [7]. It is obvious that the IGBT is switched ON during the time *[0; αT]* and diode is ON during time *[αT; T]*. Finally, conduction losses in IGBT (resp. diode) are expressed in (6) (resp. (7)).

$$P_{cond\,,\,igbt}=\frac{1}{T}\int_{0}^{\alpha T}\left[v_{\mathrm{ce,\,sat}}.i_{load}(t)+R_{ds\,,\,on}.i_{load}^{2}(t)\right]dt=v_{\mathrm{ce,\,sat}}\alpha.I_{load}+R_{ds\,,\,on}\alpha.I_{load}^{2} \tag{6}$$

$$P_{cond\,,\,diode}=\frac{1}{T}\int_{\alpha T}^{T}\left[v_{\mathrm{d0}}.i_{load}(t)+R_{d0}.i_{load}^{2}(t)\right]dt=v_{\mathrm{d0}}(1-\alpha).I_{load}+R_{d0}(1-\alpha).I_{load}^{2} \tag{7}$$

Switching losses

For the calculus of switching losses, current increase and decrease in semiconductors are considered to be linear during switching time [7]. Switching losses appear in IGBT due to controlled commutations. Power losses during turn-on time t_{on} are mainly due to the simultaneous presence of voltage and current in the component and to the charging of internal capacitance C_{oss}. The considered current takes into account the load current and the reverse recovery current of the diode I_{rm}. Note that effects due to parasitic inductance and neglected. During turning-off time t_{off}, switching losses in the IGBT are only due to the simultaneous presence of voltage and current in the component.

Finally, switching losses in diode only occur during turn-off due to reverse recovery current. It takes into account the integral of current Q_{rr} when voltage appears in the component. Expressions (8) summarize the three cases of switching losses previously described.

$$\begin{cases} P_{\text{on, igbt}} = \left[\dfrac{E.(I_{load} + I_{rm})}{2} .t_{on} + \dfrac{2}{3} C_{oss} .E^2 \right] f \\ P_{\text{off, igbt}} = \dfrac{E.I_{load}}{2} .t_{off} .f \\ P_{\text{off, diode}} = E.Q_{rr} .f \end{cases} \tag{8}$$

Diode and IGBT losses

Equations (6), (7) and (8) allow to compute power losses in semiconductors regarding operating conditions. Figure 4 illustrates the power losses regarding duty cycle α.

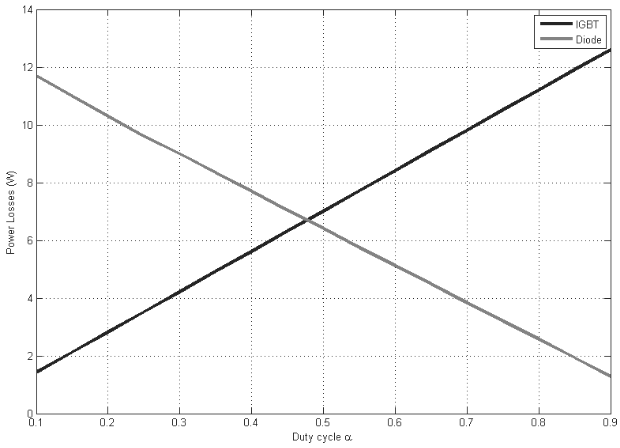

Fig. 4: Power losses in semiconductors

Based on such results, a linear approximation of power losses is expressed in (9).

$$\begin{cases} P_{\text{igbt}} = 13.98\alpha + 0.026 \\ P_{\text{diode}} = -12.93\alpha + 12.89 \end{cases} \tag{9}$$

The power losses of the IGBT when the duty cycle tends to *0* corresponds to the switching losses since no current flows through the component. Similarly, the limit case where the diode is not submitted to any current (equivalently, when the duty cycle approaches *1*) provides the switching losses within this component. It can be seen that switching losses in the diode are lower than those in the IGBT. This stands in agreement with the uncontrolled characteristics of the diode switching and also with the technological difference between these two components.

Moreover, it seems that such a difference in the technology of semiconductors also leads to distinct power losses dependency regarding duty cycle. This may be explained by the lower on-state resistance of the SiC diode, which induces a reduction in conduction losses.

Total power losses and efficiency

In order to demonstrate the overall efficiency of our integrated assembly, complementary studies about losses of passive elements are expressed. Passive elements of the chopper converter are defined as power tracks, Aluminium wire bondings and brazing. Power losses in these elements are only due to Joule effect. Electric resistance R of materials are evaluated through their own resistivity ρ, their length l and section S (10). Moreover, the RMS current in each passive element is set either to the RMS current in the IGBT ($\sqrt{\alpha}.I_{load}$) or in the diode ($\sqrt{1-\alpha}.I_{load}$).

$$R = \frac{\rho.l}{S} \tag{10}$$

Considering all power losses in the studied converter, the efficiency of electric conversion may be estimated. It can be established from the model that the overall efficiency is around *82.4% ± 0.5%* along the whole range of duty cycle. Experimental measurements indicates an efficiency of *83.5%* for $\alpha=0.5$ leading to a validation of the previous losses study.

Thermal model

Previous power losses model leads to local heat production in the system. Consequently, a thermal model of the converter, linked to heat sources, has to be established for local component temperature monitoring.

Electro-thermal analogy

In order to model the thermal behaviour of the converter, the differential form of Fourier's law of thermal conduction is considered (11) [8].

$$\vec{\varphi} = -k.\overrightarrow{grad}\,T \qquad (11)$$

where:

- $\vec{\varphi}$ is the heat flux density
- k is the thermal conductivity
- T is the temperature

This behaviour is similar to the electrical one if the Ohm's law is under consideration. Indeed, equivalent thermal parameters are defined by using analogy as given in table I [9].

Table I: Electro-thermal analogy

Thermal element	Electrical element
Temperature (*K*)	Electric potential (*V*)
Thermal flux (*W*)	Current (*A*)
Thermal resistance (*K/W*)	Resistance (Ω)
Heat capacity (*J/K*)	Capacity (*F*)

For the material set used, thermal parameters, resistance R_{th} and capacity C_{th}, are evaluated using (12) [10]. Moreover, link with ambient temperature is achieved with convection resistance R_{cv}.

$$\begin{cases} R_{\mathrm{th}} = \dfrac{l}{\lambda S} \\ C_{\mathrm{th}} = \mu.V.C_p \\ R_{cv} = \dfrac{1}{h.S} \end{cases} \qquad (12)$$

where:

- l is the length of the thermal path in m
- λ is the thermal conductivity in $W.K^{-1}.m^{-1}$
- S is the cross section of the thermal path in m^2
- μ is the volumetric mass density of the material in $kg.m^{-3}$

- V is the volume of the material in m^3
- C_p is the heat capacity per mass in $J.K^{-1}.kg^{-1}$
- h is the coefficient of convection in $W.K^{-1}.m^{-2}$

Elementary thermal models

Due to the various geometry and thermal behaviour of the designed components, several thermal models are designed. They will be finally linked to produce an overall thermal model connected to electrical inputs.

One dimension model

Let's consider a one dimension system that conducts thermal flux. A heat source is included in the system. The associated electro-thermal model is depicted in figure 5-a. The heat source and heat capacity reflects a global behaviour of the system. Moreover, convection effects are also considered and applied. As a contrary, thermal resistances depict local behaviour by given temperature in a specific location that may be selected by setting values of resistances. Note that the sum of local thermal resistances equals the total thermal resistance of the system in the considered dimension.
This model is suitable for elements of the chopper converter such as bonding wires due to the ratio between their length and their section.

Three dimensions model

The three dimensions thermal model is an extension of the one dimension model. The difference lies in the position of convection resistance. Indeed, heat transfer related to convection is applied on surfaces. Consequently, convection resistance are linked (if applicable) on external nodes of the model as illustrated in figure 5-b. This model is suitable for power tracks, power chips, substrate and brazing.

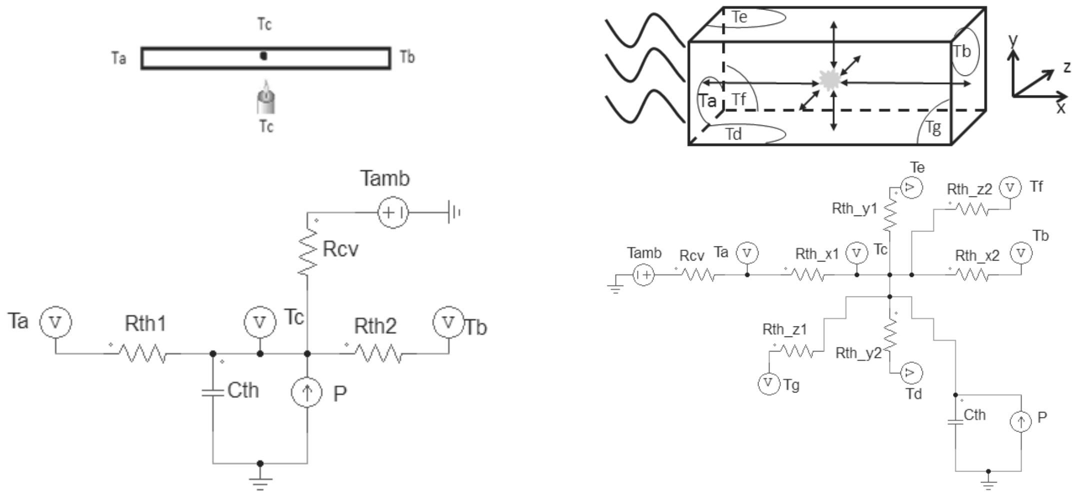

(a) – One dimension thermal model (b) – Three dimensions thermal model

Fig. 5: Electro-thermal elementary models

Thermal model of the chopper converter

In order to build the thermal model of the whole converter, it is necessary to define cells thermally linked together. These cells are composed of several materials dispatched in several layers. Each material is represented by a three dimension thermal model. According to thermal losses study, heat source are placed on the different models if necessary.

Regarding chopper converter geometry in figure 1-b, twelve thermal cells are defined as presented in figure 6-a. They are delimited by dot lines. Moreover, three cells are also defined for wire bonding connections. Figure 6-b indicates how is built the thermal model of the cell which concerns the IGBT. It is thermally linked to adjacent cells by substrate, copper tracks and wire bondings. It can be noticed that convection effects are neglected on cross section of copper tracks, IGBT and brazing.

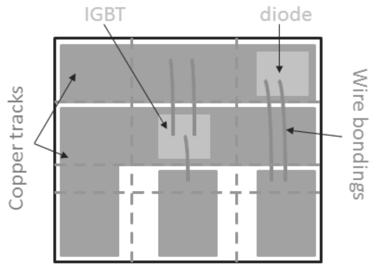

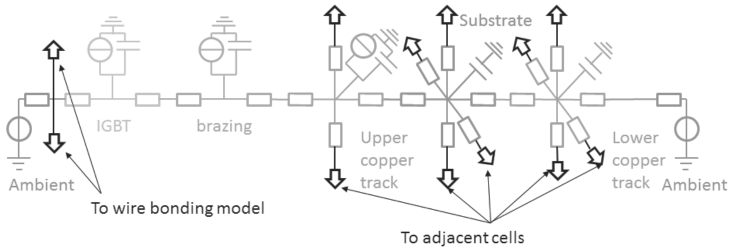

(a) – Thermal cells definition (b) – Thermal model of IGBT cell

Fig. 6: Thermal model of the chopper converter

Simulation results

Thermal elevation of power chips is computed regarding duty cycle α at constant load current $I_{load}=8A$ using heat dissipations previously determined. Simulation results are given in figure 7. Semiconductor temperature is compared to ambient one to obtain thermal elevation. It can be seen that thermal elevation of IGBT (resp. diode) increase (resp. decrease) with duty cycle as well as heat losses. Moreover, in figure 7, it seems that temperature elevation of components is not strictly correlated with heat source analysis provided in figure 4.This may be due to the geometry of the assembly. Indeed, IGBT chip is surrounded by Copper tracks that facilitate thermal transfer from the power chip to the environment. Finally, it may be concluded that geometry of assemblies has to be strongly studied for cooling systems design and temperature operating point of power semiconductors. Indeed, this study could allow to determine and optimize leading geometry parameters inducing Joule losses such as conductions paths.

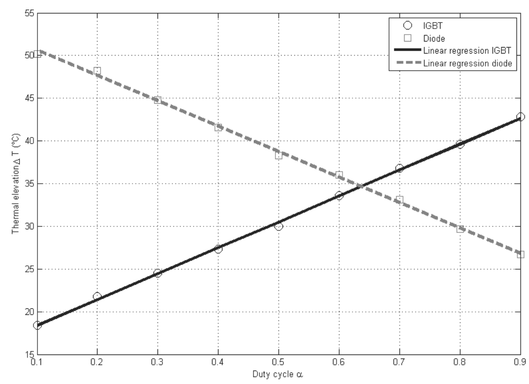

Fig. 7: Thermal elevation of semiconductors

Conclusion

In this work, heat sources linked to Joule effect losses has been identified. The interest of a hybrid assembly between a Si controlled component and SiC un-controlled component within a buck converter has been demonstrated regarding overall efficiency. Indeed, the use of a SiC diode leads to a decrease in the overall Joule losses of the assembly, allowing a clear benefit in the design of the heat dissipation elements. Moreover, a thermal model based on geometry, heat source locations, physical links and materials properties has been built. This model allowed to determine temperature elevation in operating conditions of the different elements of the converter, especially of power chips.

Further works will deal with accurate electrical measurements in order to characterize the dissipated energy during switching of the IGBT and diode. The proposed thermal model may be used to obtain the thermal distribution along elements such as wire bonding to derive design criteria. These thermal studies will allow to examine the dissipation and cooling systems and to optimize power structures and their ageing under electro-thermal stresses. Finally, the use of causal thermal model may lead to define an observer to estimate inner temperature of power chips using external measurements.

References

[1] Funaki T., Balda J-C., Junghans J., Kashyap A-S., Mantooth H-A., Barlow F., Kimoto T., Hikihara T.: Power Conversion With SiC Devices at Extremely High Ambient Temperatures, IEEE Transactions on Power Electronics, Vol. 22, no 4, pp. 1321-1329, 2007

[2] Ye H., Lin C., Basaran C.: Failure modes and FEM analysis of power electronic packaging, Finite Elements in Analysis and Design, Vol. 38, pp. 601-612, 2002

[3] Smet V., Forest F., Huselstein J-J., Richardeau F., Khatir Z., Lefebvre S., Berkani M.: Ageing and Failure Modes of IGBT Modules in High-Temperature Power Cycling, IEEE Transactions on Industrial Electronics, Vol. 58, no 10, pp. 4931-4941, 2011

[4] Chen M., Hu A., Yang X.: Predicting IGBT Junction Temperature with Thermal Network Component Model, Power and Energy Engineering Conference, 2011

[5] Ouwerkerk D., Han T., Preston J.: Efficiency improvement using a hybrid power module in 6.6 kW non-isolated on-vehicule charger, 2012 IEEE Vehicule Power and Propulsion Conference, Seoul, 2012

[6] Baliga B. J.: Fundamentals of power semiconductor devices, Springer, 2008

[7] Rashid M. H.: Power electronics handbook - 3rd edition, Elsevier, 2011

[8] Coleman B.D., Noll W.: The thermodynamics of elastic materials with heat conduction and viscosity, Archive for Rational Mechanics and Analysis, Vol. 13, pp. 167-178, 1963

[9] Lasance C. J. M., Vinke H., Rosten H.: Thermal Characterization of Electronic Devices with Boundary Condition Independent Compact Models, IEEE transactions on components, packaging, and manufacturing technology - part A, Vol. 18, no 4, 1995

[10] Bar-Cohen A., Kraux A. D.: Advances in thermal modeling of electronic components and systems, ASME Press, 1988